

GAILDUNNINGITE, IDEALLY $\text{Hg}^{2+}_3[\text{NHg}^{2+}_2]_{18}(\text{Cl},\text{I})_{24}$, A NEW MINERAL FROM THE CLEAR CREEK MINE, SAN BENITO COUNTY, CALIFORNIA, USA: DESCRIPTION AND CRYSTAL STRUCTURE

MARK A. COOPER AND FRANK C. HAWTHORNE[§]

Department of Geological Sciences, University of Manitoba, Winnipeg, Manitoba R3T 2N2, Canada

ANDREW C. ROBERTS

Geological Survey of Canada, 601 Booth Street, Ottawa, Ontario, K1A 0E8, Canada

CHRISTOPHER J. STANLEY AND JOHN SPRATT

Natural History Museum, London, SW7 5BD, United Kingdom

ANDREW G. CHRISTY

Geosciences, Queensland Museum, 122 Gerler Road, Hendra, Queensland 4011

School of Earth and Environmental Sciences, University of Queensland, St. Lucia, Queensland 4072, Australia

ABSTRACT

Gaildunningite, ideally $\text{Hg}^{2+}_3[\text{NHg}^{2+}_2]_{18}(\text{Cl},\text{I})_{24}$, is a new mineral from the Clear Creek mine, New Idria mining district, San Benito County, California, USA. It is orthorhombic, space group *Amam*, $Z = 4$; a 26.381(6), b 45.590(10), c 6.6840(15) Å, V 8039(5) Å³. Chemical analysis by electron microprobe gave Hg 76.87, I 12.55, Cl 3.79, Br 0.56, S 0.18 wt.%; N 2.45, O 0.28, and H 0.02 wt.% were derived from the crystal structure to give a total of 96.70 wt.%. The empirical formulae (calculated on the basis of 39.44 Hg with 18 N and OH added to give electroneutrality) is $\text{Hg}^{2+}_{39.44}\text{N}_{18}[\text{Cl}_{11.00}\text{I}_{10.18}(\text{OH})_{1.81}\text{Br}_{0.73}\text{S}_{0.58}]_{\Sigma 24.30}$ and the simplified formula is $\text{Hg}^{2+}_3[\text{NHg}^{2+}_2]_{18}(\text{Cl},\text{I})_{24}$. The seven strongest lines in the X-ray powder diffraction pattern [listed as d (Å), l , (hkl)] are as follows: 2.853, 100, (880, 0.16.0); 2.776, 100, (462, 5.14.0); 2.745, 100, (542); 5.717, 50, (440, 080); 5.965, 40, (131); 5.018, 40, (331); 1.673, 40, (004). Gaildunningite generally forms complex parallel intergrowths of fibrous to acicular crystals elongated along [001]. Acicular yellow to orange to darker orange-red crystals up to 0.1 mm long form matted nests lining vugs within white-grey quartz. Gaildunningite has a vitreous to adamantine luster, is transparent, and does not fluoresce under short- or long-wave ultraviolet light. Mohs hardness \approx 3 and the calculated density is 8.22 g/cm³. It is brittle with an uneven fracture and has very good cleavage on {100} and {010} and good cleavage on {001}; neither parting nor twinning was observed. It is grey in reflected light with possibly minor birefractance but no reflectance pleochroism, and strong yellow-orange internal reflections are evident even in plane-polarized light. The Raman spectrum indicates the presence of Hg–N bonds in the structure. The crystal structure of gaildunningite is based on a well-ordered three-dimensional $[\text{NHg}_2]^+$ net of near-linear N–Hg–N groups, where each N^{3-} is tetrahedrally coordinated by Hg^{2+} . The net is comprised of two five-membered, three six-membered, one seven-membered, and one eight-membered rings of N–Hg–N groups. The interstitial part of the structure is significantly disordered and consists of (Hg^{2+}) and ($\text{I}, \text{Cl}, \text{Br}, \text{S}^{2-}, \text{OH}$) ions. A new bond-valence parameter has been derived for (Hg^{2+} – N^{3-}) bonds: $R_0 = 1.964$ Å, $b = 0.37$; this gives bond-valence sums at the N^{3-} ions in accord with the valence-sum rule.

Gaildunningite and unnamed CCUK-18 are the only (Hg–N–I)-bearing minerals discovered at Clear Creek to date and are closely associated; gaildunningite is the later of these two minerals and tends to grow on CCUK-18. They post-date the iodine-free nitride mosesite and the (N,I)-free chlorides such as eglestonite, implying that iodine was a late addition to the overall chemical system. Both the mineral and the mineral name have been approved by the Commission on New Minerals, Nomenclature and Classification of the International Mineralogical Association (IMA 2018–029). The mineral is named after Gail E. Dunning (b. 1937), a prominent field-collector of minerals from the New Idria mining district who has been responsible for the discovery of many new mercury-bearing minerals.

[§] Corresponding author e-mail address: frank_hawthorne@umanitoba.ca

Keywords: gaildunningite, new mineral, mercury-nitride-chloride-iodide, crystal-structure refinement, infrared spectrum, Raman spectrum, electron-microprobe analysis, Hg–N bond-valence parameters, Clear Creek mine, San Benito County, California.

DEDICATION

This work is dedicated to the memory of Gail's longtime mineral-collecting colleague Joseph F. (Fen) Cooper, Jr. (1937–2017).

INTRODUCTION

The Clear Creek mine, San Benito County, California, USA, has been an abundant source of new and rare Hg-bearing minerals (Dunning *et al.* 2005). As part of our continuing interest in Hg-bearing minerals (Hawthorne *et al.* 1994, Cooper & Hawthorne 2003, 2009, Cooper *et al.* 2013, 2016, Roberts *et al.* 1981, 1996, 2001, 2002, 2003a, b, 2004, 2005), here we report on a new mercury-nitride-chloride-iodide mineral from the Clear Creek mine. The new mineral is named after Mr. Gail E. Dunning (born 1937) of Sunnyvale, California, who recognized the mineral in 1993 at the Clear Creek mercury mine, San Benito County, California, USA. Mr. Dunning, now a retired metallurgical engineer formerly with General Electric Company, has been an avid collector of rare minerals since 1957, specializing in barium-silicate and mercury-bearing minerals. To date, he has discovered over 20 new or potentially new minerals which are currently under study. He has authored or co-authored 48 papers relating to new mineral descriptions and mineralization of California and Nevada mines. The holotype specimen of gaildunningite has been deposited in the collections of the Department of Natural History (Mineralogy), Royal Ontario Museum, 100 Queens Park, Toronto, Ontario M5S 2C6, Canada (catalogue number M58523) and the Natural History Museum, London, SW7 5BD, United Kingdom (catalogue number BM 2018,100).

OCCURRENCE

Gaildunningite was recovered in 1993 from a quartz vein in float rock from the lower workings of the long-abandoned Clear Creek mine (120°43'58"W, 36°22'59"N) (Fig. 1), located within the New Idria mining district, San Benito County, California, USA (Dunning *et al.* 2005). Beginning with the discovery of cinnabar at New Idria in 1853, smaller mercury-bearing deposits were discovered in the Clear Creek area to the southwest (Bradley 1918, Eckel & Myers 1946, Linn 1968). The Hg-bearing zones in the Clear Creek area are situated along a NW–SE trend of shallow, randomly exposed silica-carbonate orebodies that are underlain by

unaltered serpentinite. These shallow tabular orebodies of ocherous silicified rock represent discontinuous remnants of a low-angle shear zone dipping gently to the southwest (Eckel & Myers 1946). Sporadic operation of these surface workings continued until recorded production ended in 1942 (Linn 1968). The history of mineral collecting at the Clear Creek mine extends back to at least 1959 with the discovery by Mr. Edward H. Oylar of a mercury mineral that eventually was named in his honor, edoylerite, and this has been followed by numerous additional discoveries of new mercury minerals (Dunning *et al.* 2005). Gaildunningite (previously designated as CCUK-10) occurs in massive quartz, generally closely associated with another (Hg–N)-bearing mineral (CCUK-18), which may be an iodine analogue of mosesite according to powder diffraction and SEM-EDS data (Dunning *et al.* 2005). The New Idria serpentinite body is thought to be a tectonically emplaced section of late-Jurassic Pacific oceanic crust, and metamorphism of surrounding sediments released Hg-bearing fluids that migrated along fractures within the silicified serpentinite and produced the mercury mineralization (Studemeister 1984). The primary mercury minerals seem to have been cinnabar, metacinnabar, and donharrissite, but these reacted to produce a diverse range of secondary species in response to changing fluid composition. Different assemblages are preserved in cavities that in effect became sealed reaction vessels that sampled the associated fluid at different points during its evolution through time. Gaildunningite and CCUK-18 are the only Hg–N–I minerals discovered at Clear Creek to date and are closely associated, with gaildunningite the later of the two and tending to grow on CCUK-18. They post-date the iodine-free nitride mosesite and CCUK-19 and the (N,I)-free chlorides such as eglestonite, implying that iodine was a late addition to the overall chemical system (Dunning *et al.* 2005).

PHYSICAL PROPERTIES

Yellow to orange to darker orange-red acicular gaildunningite crystals (Fig. 2a) form matted nests lining vugs within white-grey quartz (Fig. 2b). Individual crystals are up to 0.1 mm long with length-to-width aspect ratios of ~100:1 or greater. Crystals are elongated along [001], with possible {100} and {010} pinacoids occurring on rare isolated fibers, but more commonly gaildunningite forms



FIG. 1. View of the general area of the Clear Creek mine, lower workings, where the few samples of gaildunningite were discovered. Photographer: Gail Dunning.

complex parallel intergrowths (Figs. 2a, 3). Dunning *et al.* (2005) described the color as ranging further to bright yellow. Gaildunningite has an orange streak, vitreous to adamantine luster, is transparent, and does not fluoresce under short- or long-wave ultraviolet light. The Mohs hardness is ≈ 3 and the calculated density is 8.22 g/cm^3 using the chemical analysis and the cell dimensions derived from single-crystal X-ray diffraction. It is brittle with an uneven fracture and has very good cleavage on $\{100\}$ and $\{010\}$ and good cleavage on $\{001\}$; no parting or twinning was observed. The $a:b:c$ ratio calculated from the single-crystal unit-cell parameters is $0.5787:1:0.1466$.

The mineral is grey in reflected light with possibly minor bireflectance but no reflectance pleochroism. However, strong yellow-orange inter-

nal reflections are evident even in plane-polarized light. In crossed polars, these internal reflections mask both the degree of anisotropy and the anisotropic rotation tints. No grains were suitable for quantitative reflectance measurement. By analogy with comancheite ($n_{\text{meas.}} = 1.78\text{--}1.79$, Roberts *et al.* 1981), gaildunningite is expected to have a comparable refractive index, as the chemical composition, structure, and densities are similar.

INFRARED SPECTROSCOPY

An unpolarized single-crystal FTIR spectrum (Fig. 4) was recorded with a Bruker Hyperion 2000 IR microscope interfaced to a Tensor 27 spectrometer. Spectra in the range $4000\text{--}430 \text{ cm}^{-1}$ were obtained by averaging 150 scans with a resolution of 4 cm^{-1} . A

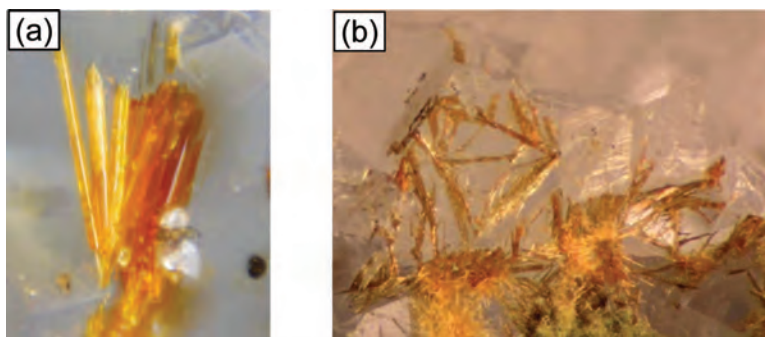


FIG. 2. Crystals of gaildunningite. (a) A bundle of radiating acicular yellow and orange-red crystals; the crystal group is $250 \mu\text{m}$ high. (b) Dispersed crystals.

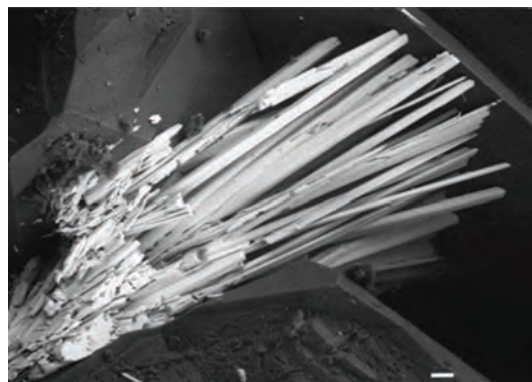


FIG. 3. SEM image of the original group of gaildunningite crystals discovered in a quartz cavity from the lower workings, Clear Creek mine.

broad envelope centered at $\sim 3395\text{ cm}^{-1}$ and a peak at $\sim 1630\text{ cm}^{-1}$ (Fig. 4) are indicative of H_2O that the crystal structure indicates must be adsorbed on the sample and present in the atmosphere. There is a shoulder on the $\sim 3395\text{ cm}^{-1}$ absorption at 3600 cm^{-1} that may be assigned to $(\text{OH})^-$. The strong peaks at 688, 652, and 579 cm^{-1} are assigned to $\text{Hg}^{2+}\text{-N}^{3-}$ stretching vibrations (Cooper *et al.* 2013).

RAMAN SPECTROSCOPY

Raman spectra in the range $100\text{--}1200\text{ cm}^{-1}$ were collected in back-scattered mode using a HORIBA Jobin Yvon-LabRAM ARAMIS integrated confocal micro-Raman system equipped with a 460 mm focal-length spectrograph and a multichannel air-cooled (-70°C) CCD detector. A magnification of 1006 was used with an estimated spot size of $\sim 1\text{ mm}$, an 1800 gr/mm grating, and a 785 nm excitation laser. The

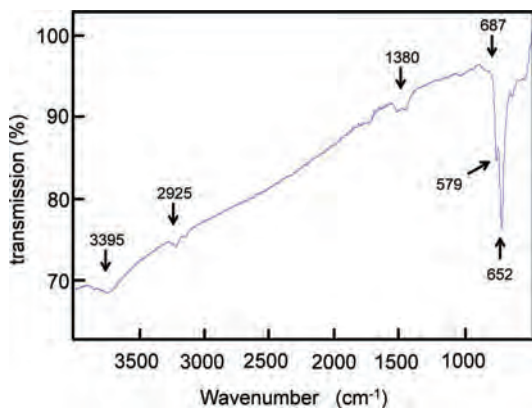


FIG. 4. Infrared spectrum of gaildunningite.

TABLE 1. CHEMICAL DATA (wt.%) FOR GAILDUNNINGITE

Constituent	Mean	Range	Stand. Dev.
Hg	76.87	75.90–78.30	0.70
N	2.45*		
I	12.55	10.60–15.60	1.06
Cl	3.79	2.81–4.28	0.30
Br	0.56	0.38–0.75	0.09
S	0.18	0.01–0.37	0.09
O	0.28*		
H	0.02*		
Total	96.70		

* Calculated (see text)

wavenumber was calibrated using the 520.7 cm^{-1} line of elemental Si. The spectroscopic discrimination of O^{2-} and N^{3-} in Hg^{2+} compounds can be made in the $350\text{--}700\text{ cm}^{-1}$ range of a Raman spectrum, with $\text{Hg}^{2+}\text{-O}^{2-}$ stretching vibrations occurring from $350\text{--}500\text{ cm}^{-1}$ and $\text{Hg}^{2+}\text{-N}^{3-}$ stretching vibrations occurring from $500\text{--}700\text{ cm}^{-1}$ (Cooper *et al.* 2013). It is clear that significant Raman peaks belonging to gaildunningite occur in the $\text{Hg}^{2+}\text{-N}^{3-}$ stretching region (555 and 580 cm^{-1}) and establish N^{3-} as the major anion bonded to Hg^{2+} in gaildunningite (Fig. 5).

CHEMICAL COMPOSITION

Chemical analysis of gaildunningite was done using a Cameca SX100 electron microprobe (WDS mode, 10 kV, 4 nA, and $1\text{ }\mu\text{m}$ beam diameter). The following standards were used: HgTe (Hg), KI (I), NaCl (Cl), KBr (Br), and baryte (S). The use of baryte as a standard for S assumes an oxidation state of S^{6+} ; subsequent to the analysis, the valency of S was determined as S^{2-} , and hence there will be a minor error in the S content due to a peak shift between the calibration of the standard (S^{6+}) and the unknown (S^{2-}). Determination of N was not attempted due to the large absorption of N $K\alpha$ X-rays by the carbon coating, the lack of a suitable N standard, and peak interference from I (M lines) and Hg (high-order lines). The data were reduced using the PAP matrix-correction routine of Pouchou & Pichoir (1985). The analytical results are given in Table 1. A low beam-voltage and current were used for this analysis, as the sample is extremely beam sensitive. The empirical formula was calculated on the basis of 39.44 Hg *apfu* with 18 N *apfu* (from structure), and $(\text{OH})^-$ was added to produce electroneutrality: $\text{Hg}_{39.44}\text{N}_{18}[\text{Cl}_{11.00}\text{I}_{10.18}(\text{OH})_{1.81}\text{Br}_{0.73}\text{S}_{0.58}]_{\Sigma 24.30}$.

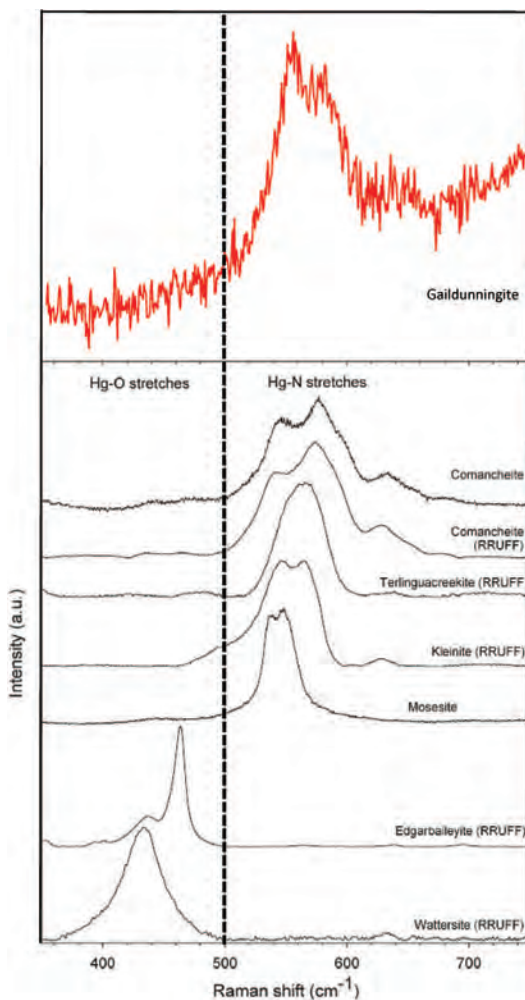


Fig. 5. Raman spectra in the range ($350\text{--}750\text{ cm}^{-1}$) of some Hg-containing minerals (reproduced from Figure 6 of Cooper *et al.* 2013) with the gaidunningite spectrum superimposed in red.

X-RAY POWDER DIFFRACTION

X-ray powder-diffraction data were collected with a 114.6 mm Debye-Scherrer powder camera using Ni-filtered Cu radiation (wavelength $\text{CuK}\alpha = 1.54178\text{ \AA}$). Intensities were estimated visually; d -spacings were not corrected for shrinkage and no internal standard was used. The cell dimensions were refined using the program CELREF (Appleman 1973) and gave the following values for an orthorhombic cell with $Amam$ symmetry: a 26.364(6), b 45.638(14), c 6.699(2) \AA . The X-ray powder-diffraction data are listed in Table 2.

X-RAY DATA COLLECTION

An acicular ($4 \times 4 \times 90\text{ }\mu\text{m}$) crystal of gaidunningite was attached to a tapered glass fiber and mounted on a Bruker D8 three-circle diffractometer equipped with a rotating-anode generator ($\text{MoK}\alpha$ X-radiation), multilayer optics, and an APEX-II CCD area detector. In excess of a Ewald sphere of diffraction data was collected to 60° 2θ using 20 s frames, a 0.2° frame width, and a crystal-to-detector distance of 5 cm. Both the mounted orientation of the crystal on the glass fiber and the orientation of the crystal relative to the incident and diffracted X-ray beam during collection of the intensity were optimized

TABLE 2. X-RAY POWDER DIFFRACTION DATA FOR GAILDUNNINGITE

$I_{\text{obs.}} \%$	$d_{\text{obs.}} \text{ \AA}$	$d_{\text{calc.}} \text{ \AA}$	hkl	$I_{\text{obs.}} \%$	$d_{\text{obs.}} \text{ \AA}$	$d_{\text{calc.}} \text{ \AA}$	hkl
5	11.444	11.414	2 2 0	3	2.283	2.286	11 6 0
		11.409	0 4 0			2.285	5 18 0
5	8.191	8.201	3 2 0			2.283	10 10 0
3	7.612	7.606	0 6 0	20	2.259	2.258	3 14 2
5	6.571	6.591	4 0 0	3	2.230	2.232	11 3 1
		6.588	2 6 0			2.232	7 15 1
40	5.965	5.972	1 3 1	10	2.200	2.202	1 3 3
50	5.717	5.707	4 4 0			2.195	9 2 2
		5.705	0 8 0			2.195	7 10 2
10	5.556	5.559	2 3 1	20	2.168	2.172	8 8 2
5	5.397	5.401	0 5 1			2.165	9 4 2
10	5.254	5.236	2 8 0	15	2.140	2.143	2 16 2
40	5.018	5.028	3 3 1			2.143	3 3 3
15	4.796	4.786	5 4 0			2.139	4 19 1
		4.785	3 8 0			2.136	5 14 2
20	4.671	4.674	4 1 1	10	2.112	2.111	12 6 0
		4.672	0 7 1	5	2.076	2.072	10 0 2
20	4.495	4.497	1 10 0	3	2.054	2.057	9 8 2
		4.489	4 3 1	20	2.020	2.022	0 18 2
20	4.317	4.315	6 2 0			2.019	3 22 0
		4.313	4 8 0	10	1.988	1.988	8 17 1
		4.313	2 10 0			1.985	9 10 2
15	4.181	4.177	4 5 1	15	1.943	1.947	6 16 2
5	4.109	4.101	6 4 0			1.942	11 2 2
10	4.000	3.998	5 3 1	3	1.925	1.925	13 3 1
		3.996	1 9 1	5	1.901	1.903	0 23 1
30	3.793	3.805	6 6 0			1.899	13 5 1
		3.803	0 12 0			1.898	11 13 1
3	3.417	3.408	6 5 1			1.898	9 17 1
5	3.354	3.350	0 0 2	20	1.882	1.886	10 10 2
15	3.293	3.295	8 0 0			1.886	0 20 2
		3.294	4 12 0			1.884	4 11 3
3	3.198	3.209	7 3 1			1.881	7 16 2
		3.208	5 9 1	5	1.861	1.865	12 11 1
		3.190	1 4 2			1.864	8 19 1
3	3.087	3.088	1 13 1	5	1.843	1.843	7 7 3
		3.085	5 12 0			1.842	5 11 3
15	3.023	3.018	3 4 2			1.842	3 13 3
3	2.991	2.986	4 0 2	10	1.826	1.831	12 2 2
		2.986	2 6 2			1.828	14 6 0
30	2.935	2.932	7 7 1	3	1.802	1.800	0 15 3
		2.932	5 11 1			1.800	9 20 0
		2.931	3 13 1	10	1.775	1.776	5 20 2
20	2.894	2.894	3 6 2	3	1.743	1.743	9 5 3
100	2.853	2.854	8 8 0			1.743	7 11 3
		2.852	0 16 0	3	1.722	1.722	13 14 0
5	2.818	2.822	2 8 2	5	1.698	1.699	15 1 1
		2.812	4 13 1			1.699	13 13 1
100	2.776	2.780	4 6 2			1.698	7 23 1
		2.773	5 14 0	5	1.686	1.686	7 20 2
100	2.745	2.744	5 4 2	40	1.673	1.675	0 0 4
35	2.690	2.686	1 10 2	10	1.653	1.654	12 12 2
30	2.639	2.636	10 0 0	25	1.637	1.637	14 2 2

TABLE 2. CONTINUED.

$l_{\text{obs.}} \%$	$d_{\text{obs.}} \text{ \AA}$	$d_{\text{calc.}} \text{ \AA}$	hkl	$l_{\text{obs.}} \%$	$d_{\text{obs.}} \text{ \AA}$	$d_{\text{calc.}} \text{ \AA}$	hkl
15	2.576	2.575	9 5 1			1.637	8 20 2
		2.574	7 11 1			1.637	6 22 2
10	2.536	2.535	0 18 0			1.636	13 15 1
30	2.491	2.488	7 2 2			1.636	1 27 1
30	2.466	2.469	2 12 2	5	1.622	1.622	13 10 2
		2.465	9 10 0	40	1.604	1.605	14 6 2
15	2.409	2.417	3 12 2			1.604	10 18 2
		2.403	5 10 2			1.604	4 24 2
15	2.371	2.372	9 9 1	5	1.579	1.577	14 8 2
3	2.350	2.349	8 0 2	30	1.545	1.545	14 10 2
		2.349	4 12 2			1.544	12 16 2
3	2.322	2.321	9 12 0				

with respect to X-ray path-lengths passing through the crystal, as this highly absorbing crystal has very significant shape anisotropy. The data-collection strategy used numerous ω - and φ -scanning runs on a 3-circle goniometer with fixed χ . The net result is a highly redundant data set that includes: (1) approximately $3\times$ full Ewald coverage and (2) robust Ψ -sampling (*i.e.*, about the diffraction vector) in relation to predictably varying path-lengths through the crystal. This purposeful sampling of various X-ray transmissivities allowed an optimal empirical absorption correction to be applied to the data. The narrow prism-shaped crystal ($4 \times 4 \mu\text{m}$ cross-section), mounted and scanned in this manner, gave reported minimum and maximum relative transmission factors of 0.0785 and 0.1553, respectively, for the empirical absorption correction. Although the unit cell contains two longer axes ($a = 26.364$, $b = 45.638 \text{ \AA}$), neighboring sharp diffraction maxima were well-resolved using a crystal-to-detector distance of 5 cm, which is a testament to the high-quality (low-mosaicity) diffracting character of the crystal used for the data collection. Thus, although the structural model includes significant disorder in relation to the interstitial constituents, this disorder does not result in any significant streaking of the diffraction maxima in the raw-data frames. A total of 157,372 reflections was integrated, empirical absorption corrections (SADABS, Sheldrick 2008) were applied, and identical reflections were averaged, resulting in 46,798 individual reflections within the Ewald sphere. This merging (following an absorption correction) of identical reflections that were collected at various Ψ -settings has an internal agreement factor of 3.48% and represents the intrinsic reproducibility of the diffraction data. In general, this high level of internal agreement can only be obtained if the following are all true: (1) the single crystal must be high quality, (2)

the reflection intensities must be adequately observed, and (3) the intensity data must be well-corrected for absorption effects. In the specific case of gaildunningite (a highly absorbing micro-crystal of very non-uniform shape), (1) was achieved after many attempts were made (over more than a decade) to try and isolate and mount a high-quality single-crystal that did not suffer from parallel-growth issues, (2) was achieved in relation to the availability of an instrument with a rotating-anode generator that produces a very intense X-ray beam, and (3) was attainable after implementing years of experience into optimal data-collection strategies for highly absorbing crystals. Analysis of the full Ewald sphere of data showed that: (1) no reflections were observed that violate the extinction conditions for an A -lattice or an a -glide plane, (2) the $|E^2 - 1|$ value of 1.029 indicates the presence of a center of symmetry, and (3) the Laue (mmm) merging result of 2.42% strongly supports the presence of orthorhombic symmetry. The combined result of (1), (2), and (3) is consistent with the space group $Amam$ (#63), and the intensity data were merged in this space group to give 6498 unique reflections ($R_{\text{merge}} = 2.42\%$); other information pertaining to data collection and refinement are given in Table 3. The crystal structure was solved in the space group $Amam$ using direct methods. Of the 6498 unique reflections, 5884 were classed as observed [$F_o > 4\sigma F$], and the structure refined to an R_1 value of 2.41%. The structure has significant disorder in much of the non- $[\text{NHg}_2]^+$ net constituents. However, further testing of lower symmetries that might possibly coincide with atom ordering is not justified given the high level of internal agreement between various indices throughout data processing and structure refinement. The final unit-cell is based on least-squares refinement of 4049 reflections ($I > 10\sigma I$). The refined model consists of an ordered $[\text{NHg}_2]^+$ net containing 15 Hg sites and 10

TABLE 3. MISCELLANEOUS CRYSTALLOGRAPHIC DATA FOR GAILDUNNINGITE

a (Å)	26.381(6)	Crystal size (µm)	$4 \times 4 \times 90$
b	45.590(10)	Radiation	MoK α
c	6.6840(15)	No. of reflections	157,372
V (Å ³)	8039(5)	No. in Ewald sphere	46,798
Space group	<i>Amam</i>	R_{merge} (%)	2.42
Z	4	No. unique reflections	6498
		No. with ($F_o > 4\sigma F$)	5884
		R_1 (%)	2.41
		wR_2 (%)	5.88
Cell content: $\text{Hg}^{2+}_3[\text{NHg}^{2+}_2]_{18}(\text{Cl},\text{I},\text{OH},\text{Br},\text{S})_{24}$			

$$R_1 = \frac{\sum(|F_o| - |F_c|)}{\sum|F_o|};$$

$$wR_2 = \frac{[\sum w(F_o^2 - F_c^2)^2 / \sum w(F_o^2)^2]^{1/2}}{w}, w = 1/[\sigma^2(F_o^2) + 0.0239 P]^2 + 289.34 P];$$

$$\text{where } P = (\max(F_o^2, 0) + 2F_c^2)/3.$$

N sites and a disordered interstitial assemblage of six Hg sites and 22 halogen sites. Atom positions and equivalent-isotropic-displacement parameters are given in Table 4, site-scattering values (Hawthorne *et al.* 1995) and site populations are given in Table 5, selected interatomic distances and angles are given in Table 6, and bond-valences are given in Table 7. A .cif may be obtained from the Depository of Unpublished Data on the MAC website [document Gaildunningite CM57, 1800080]¹.

CRYSTAL STRUCTURE

The crystal structure of gaildunningite is based on a three-dimensional $[\text{N}^3\text{-Hg}^{2+}_2]^+$ net (Fig. 6a) of near-linear $\text{N}^3\text{-Hg}^{2+}\text{-N}^3$ groups in which each N^3 is

tetrahedrally coordinated by Hg^{2+} . This is a key crystal-chemical feature of Hg-N compounds, whereby each N^3 is surrounded by four Hg^{2+} ions at distances of 2.0–2.1 Å; this cannot occur for O atoms coordinated by Hg^{2+} ions (Cooper *et al.* 2013 and references therein). Five-, six-, seven-, and eight-membered rings (of $\text{N}^3\text{-Hg}^{2+}\text{-N}^3$ groups) are seen in (001) projection, where each N^3 vertex can be seen bonded to three Hg^{2+} ions, with the fourth $\text{N}^3\text{-Hg}^{2+}$ bond projecting either above or below. Gaildunningite has a framework structure of polymerized N^3 -centered ($\text{N}^3\text{-Hg}^{2+}_4$) tetrahedra with a $\text{N}^3\text{:Hg}^{2+}$ ratio of 1:2, comparable to the SiO_2 polymorphs and $[\text{TO}_2]$ zeolites. As the net contains N^3 and Hg^{2+} , it has a net positive charge: $[\text{N}^3\text{-Hg}^{2+}_2]^+$. The $[\text{N}^3\text{-Hg}^{2+}_2]^+$ net has two distinct five-membered rings (of equipoint ranks 4

¹ The MAC website can be found at <http://mineralogicalassociation.ca/>

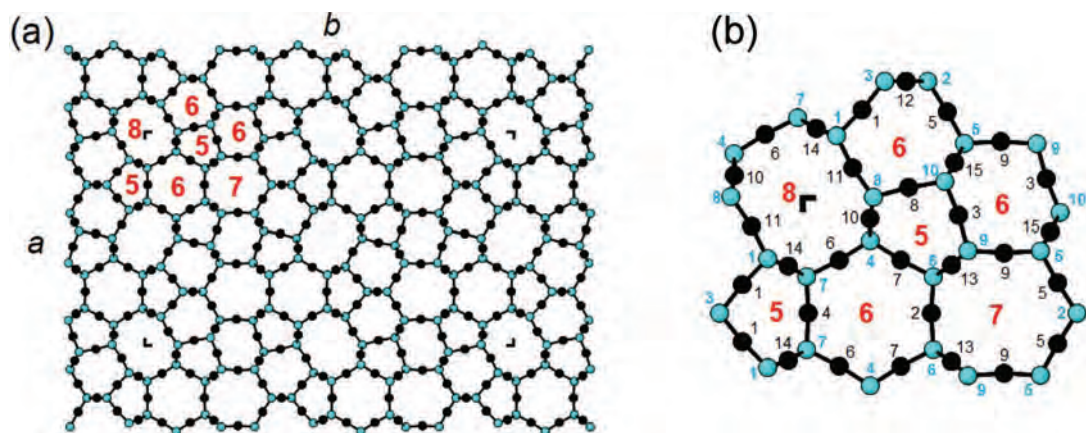


FIG. 6. The $[\text{NHg}_2]^+$ net in gaildunningite projected onto (001). (a) General connectivity between N^3 - (blue circles) and Hg^{2+} (black circles) with $[\text{N-Hg-N}]$ ring sizes labelled in red. (b) A unique part of the net with atom labels.

TABLE 4. ATOM POSITIONS AND DISPLACEMENT PARAMETERS (\AA)² FOR GAILDUNNINGITE

Site	Wyck.	x	y	z	$U_{\text{iso}}/U_{\text{eq}}$
Ordered $[\text{NHg}_2]^+$ net					
Hg1	8f	0.68828(2)	0.07477(1)	0	0.02255(8)
Hg2	4c	0.25	0.16128(1)	0.5	0.02059(11)
Hg3	8f	0.46068(2)	0.19523(1)	0	0.02212(8)
Hg4	4c	0.25	0.00750(1)	0.5	0.02088(11)
Hg5	8f	0.31593(1)	0.31891(1)	0	0.02025(8)
Hg6	8f	0.36449(2)	0.04629(1)	0.5	0.02097(8)
Hg7	8f	0.36491(2)	0.12312(1)	0.5	0.02092(8)
Hg8	8f	0.52066(2)	0.13294(1)	0	0.02226(8)
Hg9	8f	0.38008(2)	0.25200(1)	0	0.01995(8)
Hg10	16h	0.45338(1)	0.08457(1)	0.25021(4)	0.02200(6)
Hg11	8f	0.56284(2)	0.06312(1)	0	0.02248(8)
Hg12	8g	0.75	0.12975(1)	0.24994(6)	0.02186(8)
Hg13	16h	0.35445(1)	0.18655(1)	0.25078(4)	0.02058(6)
Hg14	16h	0.64799(1)	0.01744(1)	0.25034(4)	0.02252(6)
Hg15	16h	0.57450(1)	0.19029(1)	0.24970(4)	0.02098(6)
N1	8f	0.6323(3)	0.04303(16)	0	0.0116(14)
N2	4c	0.25	0.3432(3)	0	0.023(3)
N3	4c	0.75	0.1031(3)	0	0.021(3)
N4	8f	0.4066(4)	0.0850(2)	0.5	0.0209(18)
N5	8f	0.3842(3)	0.29739(17)	0	0.0155(16)
N6	8f	0.3286(4)	0.1637(2)	0.5	0.0204(18)
N7	8f	0.3289(4)	0.00560(19)	0.5	0.0196(17)
N8	8f	0.4995(4)	0.0890(2)	0	0.0218(18)
N9	8f	0.3852(3)	0.20701(18)	0	0.0172(16)
N10	8f	0.5334(4)	0.1781(2)	0	0.0224(19)
Disordered interstitial components					
Hg16	4b	0.5	0	0.5	0.0445(3)
I1	16h	0.4480(2)	0.01850(13)	0.1579(11)	0.054(2)*
C11	16h	0.4445(6)	0.0189(3)	0.305(3)	0.088(6)*
Hg17	8g	0.25	0.08749(3)	0.0573(2)	0.0485(5)
I2	4c	0.25	0.14776(3)	0	0.0297(4)
I3	8f	0.33725(4)	0.05685(2)	0	0.0334(3)
I4	4c	0.25	0.08671(3)	0.5	0.0333(5)
Hg18A	4c	0.25	0.2747(4)	0.5	0.052(5)
Hg18B	8g	0.25	0.2546(7)	0.427(3)	0.065(8)
Hg18C	16h	0.2665(7)	0.2643(6)	0.437(3)	0.065(6)
Hg19	16h	0.60467(10)	0.10374(6)	0.4477(4)	0.0513(11)
X1	8f	0.4607(12)	0.1845(9)	0.5	0.107(16)
X2	8g	0.25	0.2210(4)	0.320(5)	0.099(10)
X3	8f	0.47502(6)	0.15995(6)	0.5	0.0425(8)
X4	4c	0.75	0.06580(5)	0.5	0.0431(11)
X5	8f	0.55993(11)	0.06039(7)	0.5	0.0632(11)
X6	4c	0.75	0.01393(11)	0	0.0421(16)
X7	8f	0.39807(13)	0.13421(7)	0	0.0404(12)
X8	8g	0.25	0.24702(12)	0.1257(12)	0.077(2)
X9	4c	0.25	0.2443(3)	0	0.044(4)*
X10	8f	0.3648(4)	0.25082(15)	0.5	0.132(4)
X11	8f	0.2986(7)	0.3062(3)	0.5	0.090(5)
X12	16h	0.4735(2)	0.24104(12)	0.4022(8)	0.0370(17)
X13	8f	0.3175(15)	0.3204(13)	0.5	0.20(2)
X14	16h	0.6277(2)	0.12711(16)	0.2303(17)	0.135(5)
X15	8d	0.5	0.25	0.25	0.110(6)
X16	8f	0.6936(6)	0.0725(2)	0.5	0.065(5)
X17	8f	0.5106(8)	0.1372(5)	0.5	0.076(8)

* U_{iso}

TABLE 5. SITE ASSIGNMENTS AND SITE-SCATTERING VALUES* FOR GAILDUNNINGITE

Site	SFAC	Occupancy	<i>apfu</i>	<i>epfu</i>
Ordered [NHg ₂] ⁺ net				
Hg1	Hg	1	2	
Hg2	Hg	1	1	
Hg3	Hg	1	2	
Hg4	Hg	1	1	
Hg5	Hg	1	2	
Hg6	Hg	1	2	
Hg7	Hg	1	2	
Hg8	Hg	1	2	
Hg9	Hg	1	2	
Hg10	Hg	1	4	
Hg11	Hg	1	2	
Hg12	Hg	1	2	
Hg13	Hg	1	4	
Hg14	Hg	1	4	
Hg15	Hg	1	4	
N1	N	1	2	
N2	N	1	1	
N3	N	1	1	
N4	N	1	2	
N5	N	1	2	
N6	N	1	2	
N7	N	1	2	
N8	N	1	2	
N9	N	1	2	
N10	N	1	2	

TABLE 5. CONTINUED.

Site	SFAC	Occupancy	<i>apfu</i>	<i>epfu</i>
Disordered interstitial components				
Hg16	Hg	0.926(4)	0.926(4)	
I1	I	0.140(4)	0.560(16)	29.7(8)
Cl1	Cl	0.313(16)	1.25(6)	21.3(1.0)
Hg17	Hg	0.496(2)	0.992(4)	
I2	I	0.960(6)	0.960(6)	50.9(3)
I3	I	0.948(4)	1.896(8)	100.5(4)
I4	I	0.789(6)	0.789(6)	41.8(3)
Hg18A	Hg	0.20(2)	0.20(2)	
Hg18B	Hg	0.11(2)	0.22(4)	
Hg18C	Hg	0.109(13)	0.44(5)	
Hg19	Hg	0.1647(18)	0.659(7)	
X1	Cl	0.29(3)	0.58(6)	9.9(1.0)
X2	Cl	0.302(18)	0.60(4)	10.2(7)
X3	I	0.598(6)	1.196(12)	63.4(6)
X4	I	0.478(6)	0.478(6)	25.3(3)
X5	I	0.466(6)	0.932(12)	49.4(6)
X6	Cl	1.10(2)	1.10(2)	18.7(3)
X7	Cl	1.010(16)	2.02(3)	34.3(5)
X8	Cl	1.16(3)	2.32(6)	39.4(1.0)
X9	Cl	0.53(4)	0.53(4)	9.0(7)
X10	Cl	1.13(2)	2.26(4)	38.4(7)
X11	Cl	0.62(4)	1.24(8)	21.1(1.4)
X12	Cl	0.461(11)	1.84(4)	31.3(7)
X13	Cl	0.60(6)	1.20(12)	20(2)
X14	Cl	0.757(16)	3.03(6)	51.5(1.0)
X15	Cl	0.64(2)	1.28(4)	21.8(7)
X16	Cl	0.402(18)	0.80(4)	13.6(7)
X17	Cl	0.31(2)	0.62(4)	10.5(7)

* Hawthorne *et al.* (1995)

and 8), three distinct six-membered rings (of equipoint ranks 4, 4, and 8), one distinct seven-membered ring (of equipoint rank 4), and one distinct eight-membered ring (of equipoint rank 4) of N³⁻-Hg²⁺-N³⁻ groups (Fig. 6a) in the asymmetric part of the unit cell. This arrangement is repeated *via* a mirror plane perpendicular to the **a** axis ($x = 1/4$) and an *a*-glide plane perpendicular to the **b** axis ($y = 1/4$). The site-specific details of the rings are shown in Figure 6b. The [N³⁻Hg²⁺]⁺ net in gaildunningite is completely ordered, and all sites are fully occupied and have well-behaved anisotropic-displacement parameters. Conversely, the interstitial part of the structure has significant disorder (partly occupied sites and considerable positional disorder) of Hg²⁺ and mixed anion (Γ, Cl⁻, Br⁻, S²⁻, OH⁻) constituents. The chemical composition (Table 1) shows that Cl⁻ and Γ are the major halogens present. By comparison with comancheite, Hg²⁺₅₅N³⁻₂₄(OH,NH₂)₄(Cl,Br)₃₄ (a related structure possessing an interrupted [NHg₂]⁺ net with abundant halogens; Table 8), we expect Hg-(Cl,I) bonds in gaildunningite to have a high angle with the near-linear N³⁻-Hg²⁺-N³⁻ group (Cooper *et al.* 2013).

There are 22 halogen sites in gaildunningite; some were assigned the Γ scattering factor and some the Cl⁻ scattering factor, depending on the magnitude of the observed scattering and observed distances to neighboring Hg²⁺ ions (Table 4). The overall complexity involving partly occupied sites and positional disorder associated with the halogen sites does not allow unique assignment of site populations from the refined site-scattering values. However, the net scattering observed at all the halogen sites (expressed as e⁻) is in general agreement with that calculated from the electron-microprobe analysis, considering the overall complexity of the structure and the likely possibility of chemical variability in halogen content between different gaildunningite crystals (the crystal used for the structure was not chemically analyzed). Additional site-scattering was found at more central locations within some of the larger rings of N³⁻-Hg²⁺-N³⁻ groups. This additional scattering was assessed in three respects, (1) scattering magnitude, (2) distance to halogens coordinating the Hg²⁺ ions of the

TABLE 6. DISTANCES (Å) AND ANGLES (°) FOR THE $[\text{NHg}_2]^+$ NET ELEMENTS IN GAILDUNNINGITE

	N–Hg; Hg–N (Å)	N–Hg–N (°)
N1–Hg1–N3	2.068(8); 2.077(8)	174.0(4)
N6–Hg2–N6	2.077(9); 2.077(9)	173.9(5)
N9–Hg3–N10	2.062(9); 2.071(10)	172.9(3)
N7–Hg4–N7	2.083(9); 2.083(9)	175.2(5)
N2–Hg5–N5	2.063(8); 2.051(9)	176.1(4)
N4–Hg6–N7	2.084(9); 2.079(9)	174.6(4)
N4–Hg7–N6	2.059(9); 2.084(9)	175.0(4)
N8–Hg8–N10	2.080(10); 2.085(9)	173.7(4)
N5–Hg9–N9	2.072(8); 2.055(8)	173.2(4)
N4–Hg10–N8	2.076(6); 2.078(6)	173.9(4)
N1–Hg11–N8	2.048(7); 2.046(9)	171.4(4)
N2–Hg12–N3	2.076(8); 2.067(8)	179.7(4)
N6–Hg13–N9	2.079(6); 2.083(5)	175.3(3)
N1–Hg14–N7	2.082(4); 2.064(5)	173.7(3)
N5–Hg15–N10	2.074(5); 2.067(5)	179.9(4)
	Hg–N–Hg range (°)	<Hg–N–Hg> (°)
N1	104.5(3)–115.4(2)	109.3
N2	107.2(6)–115.0(7)	109.4
N3	103.2(6)–111.45(2)	109.5
N4	107.1(4)–115.4(4)	109.4
N5	107.4(3)–115.6(4)	109.5
N6	106.5(4)–114.3(4)	109.4
N7	107.9(4)–114.5(4)	109.4
N8	104.5(3)–115.0(3)	109.3
N9	105.0(3)–114.9(3)	109.3
N10	102.9(4)–112.6(3)	109.5

$[\text{N}^3\text{Hg}^{2+}_2]^+$ net, and (3) coordination environment of the halogens, and interpreted as resulting from the insertion of additional Hg^{2+} within the interstices of the $[\text{N}^3\text{Hg}^{2+}_2]^+$ net (a feature also observed in the structure of comancheite, Cooper *et al.* 2013).

Interstitial Hg^{2+}

The Hg16 site (Wyckoff 4b) is located within the eight-membered ring (Fig. 7). Its refined site-occupancy of 0.926(4) indicates near-full occupancy by Hg^{2+} , ideally providing one Hg^{2+} *pfu*. The neighboring electron density in the 2–3 Å range was initially modelled as a highly anisotropic single (16h) halogen site and later split into two 16h sites that were refined independently (site-scattering and isotropic displacement). The 16h site (C11) closer to the Hg16 site was assigned the Cl scattering factor and the more distant 16h site (*i.e.*, I1) was assigned the I scattering factor. The C11 site-occupancy refined to 0.313(16) and the I1 site occupancy refined to 0.140(4). On a *pfu* basis ($Z = 4$), the combined Hg^{2+} and halogen occupancies give $\text{Hg}_{0.926(4)}\text{Cl}_{1.25(6)}\text{I}_{0.560(16)}$, where the Hg:halogen ratio is near 1:2. The observed scattering sites and inferred local anion-ordering patterns are shown in Figure 7. The Hg at Hg16 is Hg^{2+} and forms disordered linear $\text{Cl}^- \text{Hg}^{2+} \text{Cl}^-$ and $\text{I}^- \text{Hg}^{2+} \text{I}^-$ groups. The observed Hg16–C11 and Hg16–I1 distances of 2.141(17) and 2.797(7) Å are in accord with these anion assignments, and the combined scattering at the C11 and I1 sites supports near-full occupancy of this interstitial region by $(\text{Cl}^- \text{Hg}^{2+} \text{Cl}^-)_{\sim 0.7} + (\text{I}^- \text{Hg}^{2+} \text{I}^-)_{\sim 0.3}$. Within a given eight-membered ring in the net along [001], the absolute orientation of the linear $\text{X}^- \text{Hg}^{2+} \text{X}^-$ group

TABLE 7. BOND VALENCES (νu)* FOR THE $[\text{NHg}_2]^+$ NET ELEMENTS IN GAILDUNNINGITE

	N1	N2	N3	N4	N5	N6	N7	N8	N9	N10	Σ
Hg1	0.75		0.74↓								1.49
Hg2						0.74→					1.48
Hg3									0.77	0.75	1.52
Hg4							0.72→				1.44
Hg5		0.77↓			0.79						1.56
Hg6				0.72			0.73				1.45
Hg7				0.77		0.72					1.49
Hg8								0.73		0.72	1.45
Hg9					0.75				0.78		1.53
Hg10				0.74↓				0.73↓			1.47
Hg11	0.80							0.80			1.60
Hg12		0.74↓	0.76↓								1.50
Hg13						0.73↓			0.72↓		1.45
Hg14	0.73↓						0.76↓				1.49
Hg15					0.74↓					0.76↓	1.50
Σ	3.01	3.02	3.00	2.97	3.02	2.92	2.97	2.99	2.99	2.99	

* Using $R_0 = 1.964$; (all arrows are $\times 2$ multipliers)

TABLE 8. A COMPARISON OF GAILDUNNINGITE AND COMANCHEITE

	Gaildunningite	Comancheite
Chemical Formula	$\text{Hg}^{2+}_3[\text{NHg}^{2+}_2]_{18}(\text{Cl}, \text{I}, \text{OH}, \text{Br}, \text{S})_{24}$	$\text{Hg}^{2+}_{55}\text{N}^{3-}_{24}(\text{OH}, \text{NH}_2)_4(\text{Cl}, \text{Br})_{34}$
Crystal System	Orthorhombic	Orthorhombic
Space Group	<i>Amam</i>	<i>Pnmm</i>
<i>a</i> (Å)	26.381	18.414
<i>b</i>	45.590	21.328
<i>c</i>	6.6840	6.6976
<i>V</i> (Å ³)	8039	2630
<i>Z</i>	4	1
Density _{meas} (g/cm ³)	–	7.7(4)
Density _{calc} (g/cm ³)	8.22	8.3
Color	Yellow to orange to orange-red	orange-red to yellow
Habit	acicular // <i>c</i>	acicular // <i>c</i>
Hg (wt.%)	76.87	86.3
I	12.55	–
Cl	3.79	6.1
Br	0.56	6.1
N*	2.45	2.6
<i>n</i> _{meas}	–	1.78–1.79
Strongest X-ray lines (<i>d</i> , <i>l</i>)	5.965(4), 5.717(5), 5.018(4), 2.853(10), 2.776(10), 2.745(10), 1.673(4)	5.68(7), 5.42(6), 2.878(8), 2.710(5), 2.669(10), 2.457(5), 1.415(5)
Locality	Clear Creek mine, California, USA	Mariposa mine, Texas, USA
References	(this work)	[1], [2]

* Calculated from structure; [1] Roberts *et al.* (1981); [2] Cooper *et al.* (2013).

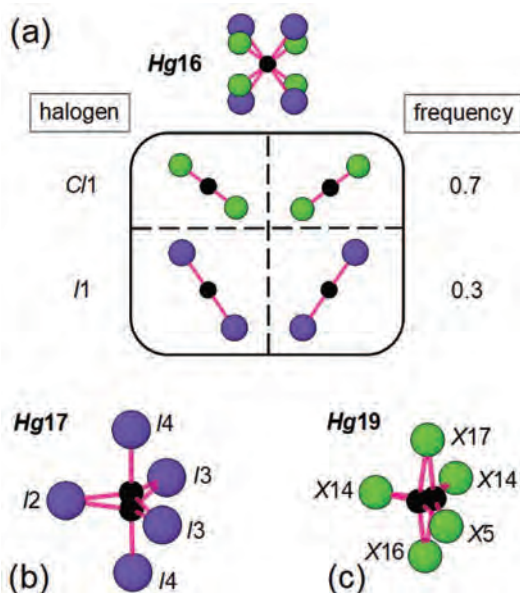


FIG. 7. The coordination environments for the interstitial Hg^{2+} in gaildunningite: (a) *Hg16*, (b) *Hg17*, (c) *Hg19*.

(X^- = unspecified halogen) must be constant (*i.e.*, have same stagger to avoid close X^- – X^- approaches between neighboring X^- – Hg^{2+} – X^- groups); however, there is no constraint with regard to similar or different halogen identities between neighboring X^- – Hg^{2+} – X^- groups. The *Hg17* site (8g) occurs within the most regular six-membered ring (Fig. 8) at [0.25; 0.08749; 0.0573], lying just off the mirror plane at [1/4; *y*; 0]. The *Hg17* site is disordered across the mirror plane with a refined site-occupancy of 0.496(2) and a *Hg17*–*Hg17'* distance of 0.766(3) Å (*i.e.*, either *Hg17* or *Hg17'* is locally occupied); thus this region of the structure is nearly fully occupied by Hg^{2+} and ideally provides one Hg^{2+} *pfu*. There are five halogen sites (*I2*, *I3* ×2, *I4* ×2) coordinating the *Hg17* site at distances from 2.720 to 3.725 Å, forming a trigonal bipyramid (Fig. 7). An analogous interstitial Hg^{2+} coordinated by halogens in a trigonal bipyramidal arrangement occurs in the crystal structure of comancheite (Cooper *et al.* 2013). The halogens at *I2* and *I3* form the three shorter (~2.7 Å) equatorial bonds and have refined site-occupancies (I scattering factor) of 0.960(6) and 0.948(4), respectively, indicating that these halogen sites are occupied almost entirely by I[–]. The *I4* and *I4'* sites lie at the apices of the trigonal bipyramid (Fig. 7) and form two distinct bonds to *Hg17* (2.96 and 3.73 Å) as a function of the *Hg17* disorder across the mirror

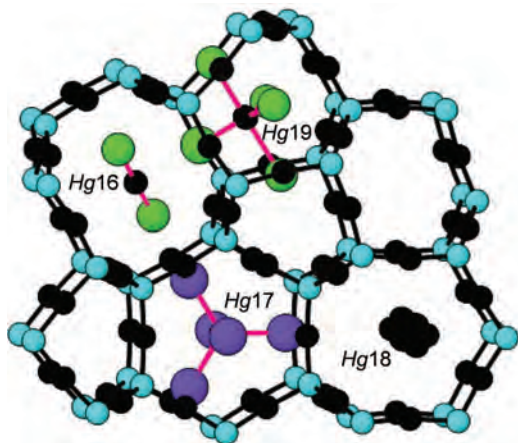


FIG. 8. Interstitial Hg^{2+} within the rings of the $[\text{NHg}_2]^+$ net in gaildunningite: $\text{Hg}16$ inside the eight-membered ring, $\text{Hg}18$ inside the seven-membered ring, and $\text{Hg}17$ and $\text{Hg}19$ inside different six-membered rings.

plane. The refined site-occupancy of 0.789(6) at $I4$ (I scattering factor) suggests that an additional lighter-scattering species (*i.e.*, Cl) is present. This interstitial region of the structure is nearly fully occupied ideally by $\text{Hg}I_5$ groups (trigonal bipyramid) (Fig. 8) that share a common $I4$ vertex to form $[\text{Hg}^{2+}I_4]$ chains along $[001]$ within the more regular six-membered rings. The $\text{Hg}18A$, $\text{Hg}18B$, and $\text{Hg}18C$ sites are close to the $4c$ position $[1/4; y; 1/2]$ where $y \approx 0.25$ and lie within ~ 1 Å of each other (Fig. 8). Collectively, the independently refined site-occupancies give a total of $0.86 \text{ Hg}^{2+} \text{ pfu}$, which is close to the ideal value of $1.0 \text{ Hg}^{2+} \text{ pfu}$ for full occupancy. The three $\text{Hg}18$ sites represent a highly disordered occupancy of the central region of the seven-membered ring by Hg^{2+} (Fig. 8). The disordered X sites ($X2$, $X8$, $X11$, $X13$) are the halogen sites coordinating the cluster of $\text{Hg}18$ sites at $\sim 2\text{--}3$ Å; however, the complexity in combined cation and anion disorder makes specific interpretation of this region of the structure quite difficult. The $\text{Hg}19$ site ($16h$) occurs within a six-membered ring and lies $0.700(6)$ Å from a neighboring $\text{Hg}19'$ site related by a mirror plane (001) at $z = 1/2$. (Figs. 7 and 8). It is surrounded by five X sites in a trigonal-bipyramidal arrangement, with the $\text{Hg}19$ position significantly off-center. The $\text{Hg}19\text{--}X$ distances range from $1.901(10)$ to $2.93(2)$ Å, with the short $\text{Hg}19\text{--}X14$ distance (1.901 Å) possibly corresponding to an $\text{Hg}^{2+}\text{--}(\text{OH})^-$ bond. For $\text{Hg}19$, the refined site-occupancy of $0.1647(18)$ indicates that this region of the structure is dominated by vacancies at the cation site, giving $(\square_{1.341}\text{Hg}^{2+}_{0.659}) \text{ pfu}$. Also, note that the apical anions at $X16$ and $X17$ (Fig. 7) both have close

approaches (< 2 Å) to neighboring $X4$ and $X3$ anions, respectively, precluding mutual local occupancy.

$\text{Hg}^{2+}\text{--}\text{N}^{3-}$ bond-valence

An updated bond-valence parameter of R_0 ($\text{Hg}^{2+}\text{--}\text{N}^{3-}$) = 1.95 Å was derived using bond-length criteria from comancheite (Cooper *et al.* 2013), which gave bond-valence sums for the tetrahedrally coordinated N^{3-} ions ranging from 2.81 to 2.94 *vu* for the five N^{3-} ions coordinated by ordered Hg^{2+} ions. The softness parameter b was set at the typical value of 0.37 Å, given the known correlation issues when trying to refine both R_0 and b (Brown & Altermatt 1985, Brese & O'Keeffe 1991). Robust refinement of both parameters is only possible from a data set containing a very wide range of bond distances (*cf.* Mills *et al.* 2009, Mills & Christy 2013). Individual $\text{Hg}^{2+}\text{--}\text{N}^{3-}$ distances in comancheite for these five N^{3-} ions span $2.03(2)\text{--}2.12(2)$ Å and shows greater bond-length dispersion and larger standard deviations than the range of $2.046(9)\text{--}2.085(9)$ Å for gaildunningite. Applying the $\text{Hg}^{2+}\text{--}\text{N}^{3-}$ bond-valence parameter to gaildunningite gives bond-valence sums at the N^{3-} ions ranging from 2.83–2.92 *vu*, close to the ideal value of 3 *vu*, but also significantly below the ideal value of 3 *vu*. As the $\text{Hg}^{2+}\text{--}\text{N}^{3-}$ distances in gaildunningite are a new set of well-determined bond lengths, we have modified the earlier bond-valence parameter R_0 to better conform with the $\text{Hg}^{2+}\text{--}\text{N}^{3-}$ distances observed in both comancheite and gaildunningite. The new bond-valence parameter of R_0 ($\text{Hg}^{2+}\text{--}\text{N}^{3-}$) = 1.964 Å gives bond-valence sums at the N^{3-} ions in comancheite (five N^{3-} ions) and gaildunningite (ten N^{3-} ions) ranging from 2.89 to 3.03 and from 2.92 to 3.02 *vu*, respectively (Table 6). As the N^{3-} ions in both structures receive no additional bond-valence from any other cations, this updated bond-valence parameter of R_0 ($\text{Hg}^{2+}\text{--}\text{N}^{3-}$) = 1.964 Å is expected to improve agreement with the valence-sum rule for N^{3-} ions.

CHEMICAL FORMULA

The gaildunningite structure contains a well-ordered $\text{Hg}^{2+}\text{--}\text{N}^{3-}$ net that is stuffed with disordered Hg^{2+} and halogen (Cl, I, Br) along with minor S (possibly as S^{2-}) and $(\text{OH})^-$. The structure provides an accurate N^{3-} -content and a good estimate of the Hg^{2+} content (*i.e.*, the sum of ordered Hg^{2+} in the $\text{Hg}^{2+}\text{--}\text{N}^{3-}$ net plus the refined occupancies of the disordered interstitial Hg sites). Note that all Hg in gaildunningite is clearly present as Hg^{2+} and not Hg^+ , as the latter would occur as distinctive $\text{Hg}^+\text{--}\text{Hg}^+$ dimers with characteristic $\text{Hg}\text{--}\text{Hg}$ separations of ~ 2.5 Å (Cooper & Hawthorne 2003). However, the complexity associated with significant halogen disorder (both posi-

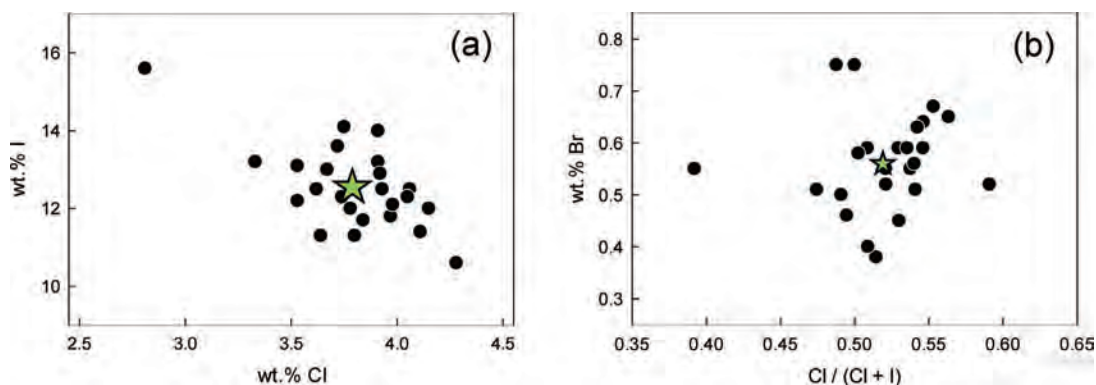


FIG. 9. Variation in halogen content for the 24 electron-microprobe point analyses of gaidunningite; green star: average analysis. (a) Iodine (wt.%) as a function of Cl (wt.%). (b) Bromine (wt.%) as a function of Cl/(Cl+I).

tional and compositional) does not allow simple assessment of the halogen content *via* structure refinement. The chemical data was therefore normalized using the Hg^{2+} and N^{3-} contents derived from the structure refinement (*i.e.*, 39.44 Hg^{2+} , 18 N^{3-} ; Table 4), with $(\text{OH})^-$ added to attain charge balance. The presence of minor $(\text{OH})^-$ is inferred from the following: (1) a minor oxygen peak observed in a wavelength-spectrometer scan during electron-microprobe analysis, (2) a minor absorption band observed at 3395 cm^{-1} in the infrared spectrum, and (3) the relatively short $\text{Hg}19\text{--}X14$ distance of 1.901 Å. This normalization results in an anion content [$\text{Cl}^- + \text{I}^- + \text{Br}^- + \text{S}^{2-} + (\text{OH})^-$] of 24.30 *apfu*, which gives a calculated site-scattering value of 776 e. The sum of the refined site-scattering values over the 22 halogen sites in the structure is 712(16) e^- (Tables 3 and 4). At the later stages of structure refinement, significant effort went into modelling the numerous residual peaks in the difference-Fourier map as disordered partly occupied halogen sites. The low final R_1 value of 2.41% suggests reasonable parity between the final structure model and the X-ray data, but the refinement end-point was far less evident than usual (*i.e.*, relative to that of an ordered structure). Many weak peaks remain in the final difference-Fourier map in the vicinity of the interstitial halogens, indicating that additional minor scattering in the data has not been fully incorporated into the structure model. Attempts to further extend the model to include this scattering were unsuccessful, due to high correlation with the existing model and general instability during least-squares refinement. We therefore regard the lower observed scattering from the halogen sites (*i.e.*, 712 e) to be due in part to less-than-ideal modelling in the structure refinement due to the significant disorder present.

Gaidunningite also shows chemical variation with respect to its halogen ratio; an earlier-analyzed sample gave $\text{Cl}_{12.89}\text{I}_{5.99}\text{Br}_{3.04}$ (when adjusted to an analogous $\text{Cl}^- + \text{I}^- + \text{Br}^-$ total) and would produce significantly less overall calculated scattering (*i.e.*, 643 e^-) for its halogen content. The reported chemical composition (Table 1) is from 24 point-analyses acquired from three crystals adjacent to the crystal used for the X-ray single-crystal work. Thus we may also attribute the discrepancy in calculated halogen scattering (EMPA) and the observed scattering (SREF) to the X-ray crystal having relatively lower I-content (and less overall halogen scattering) relative to the three crystals analyzed by electron microprobe. For the 24 chemical analyses, the variation in I and Cl shows a well-defined inverse relation (Fig. 9a). Minor Br is present (0.38–0.75 wt.%), and this Br content is shown as a function of atomic Cl/(Cl+I) in Figure 9b. It is clear from Figure 9 that several of the data points are from areas of the crystal with nearly equal Cl and I contents. The green star marking the average halogen composition falls within the Cl-dominant region, and gaidunningite is therefore defined with the dominant halogen as Cl. Additionally, Cl dominance is inferred for the X-ray single-crystal in that its aggregate scattering (*i.e.*, 712 e^-) from the halogen sites is significantly less than average calculated scattering from EMP analysis (*i.e.*, 776 e^-). The single data point plotting with the lowest Cl/(Cl+I) value in Figure 9b is presumed to have come from a crystal region with I as the dominant halogen. We strongly suspect that the gaidunningite color variation (yellow to orange to red) reflects increasing I content. The ideal formula $\text{Hg}_3^{2+}[\text{NHg}_2^{2+}]_{18}(\text{Cl},\text{I})_{24}$ shows the prevalent halogen dominance (*i.e.*, $\text{Cl}^- > \text{I}^-$) and also differentiates the ordered net component (*i.e.*, $[\text{NHg}_2^{2+}]_{18}$) from the disordered interstitial components. Of the four local interstitial regions occupied

by Hg^{2+} ions, three ($Hg16$, $Hg17$, $Hg18$) are predominantly occupied by Hg^{2+} (Hg^{2+} occupancy spans 0.86–0.99), whereas the fourth site ($Hg19$) is predominantly occupied by vacancy. Full occupancy of the interstitial ($Hg16$, $Hg17$, $Hg18$) regions ideally provides $Hg^{2+}_3 pfu$.

ACKNOWLEDGMENTS

We thank the reviewers for their comments. Financial support for this work came from the Natural Sciences and Engineering Research Council of Canada in the form of a Canada Research Chair in Crystallography and Mineralogy, a Discovery grant to FCH, and Canada Foundation for Innovation grants to FCH.

REFERENCES

- APPLEMAN, D.E. (1973) Job 9214: Indexing and Least-squares Refinement of Powder Diffraction Data. United States Geological Survey, Computer Contribution 20, United States National Technical Information Service, Document PB-16188.
- BRADLEY, W.W. (1918) Quicksilver resources of California. *California State Mining Bureau Bulletin* **78**, 20–29, 98–99.
- BRESE, N.E. & O'KEEFFE, M. (1991) Bond-valence parameters for solids. *Acta Crystallographica* **B47**, 192–197.
- BROWN, I.D. & ALTERMATT, D. (1985) Bond-valence parameters obtained from a systematic analysis of the Inorganic Crystal Structure Database. *Acta Crystallographica* **B41**, 244–247.
- COOPER, M.A. & HAWTHORNE, F.C. (2003) The crystal structure of vasilyevite, $(Hg_2)^{2+}_{10}O_6I_3(Br,Cl)_3(CO_3)$. *Canadian Mineralogist* **41**, 1173–1181.
- COOPER, M.A. & HAWTHORNE, F.C. (2009) The crystal structure of tedhadleyite, $Hg^{2+}Hg^{1+}_{10}O_4I_2(Cl,Br)_2$, from the Clear Creek Claim, San Benito County, California. *Mineralogical Magazine* **73**, 227–234.
- COOPER, M.A., ABDU, Y.A., HAWTHORNE, F.C., & KAMPF, A.R. (2013) The crystal structure of comancheite, $Hg^{2+}_{55}N^{3-}_{24}(OH,NH_2)_4(Cl,Br)_{34}$, and crystal-chemical and spectroscopic discrimination of N^{3-} and O^{2-} anions in Hg^{2+} compounds. *Mineralogical Magazine* **77**, 3217–3237.
- COOPER, M.A., ABDU, Y.A., HAWTHORNE, F.C., & KAMPF, A.R. (2016) The crystal structure of gianellaite, $[(NH_2)_2](SO_4)(H_2O)_x$, a framework of $(NH_2)_4$ tetrahedra with ordered (SO_4) groups in the interstices. *Mineralogical Magazine* **80**, 869–875.
- DUNNING, G.E., HADLEY, T.A., CHRISTY, A.G., MAGNASCO, J., & COOPER, J.F., JR. (2005) The Clear Creek mine, San Benito County, California – a unique mercury locality. *Mineralogical Record* **36**, 337–363.
- ECKEL, E.B. & MYERS, W.B. (1946) Quicksilver deposits of the New Idria district, San Benito and Fresno Counties, California. *California Journal of Mines and Geology* **42**, 81–124.
- HAWTHORNE, F.C., COOPER, M., & SEN GUPTA, P.K. (1994) The crystal structure of pinchite, $Hg_5Cl_2O_4$. *American Mineralogist* **79**, 1199–1203.
- HAWTHORNE, F.C., UNGARETTI, L., & OBERTI, R. (1995) Site populations in minerals: terminology and presentation of results of crystal-structure refinement. *Canadian Mineralogist* **33**, 907–911.
- LINN, R.K. (1968) New Idria mining district. In *Ore deposits of the United States, 1933–1967*, the Graton-Sales Volume (J.D. Ridge, ed.). American Institute of Mining, Metallurgical, and Petroleum Engineers, Inc., New York City, New York, United States (1624–1649).
- MILLS, S.J. & CHRISTY, A.G. (2013) Revised values of the bond valence parameters for $TeIV-O$, $TeVI-O$, and $TeIV-Cl$. *Acta Crystallographica* **B69**, 145–149.
- MILLS, S.J., CHRISTY, A.G., CHEN, E.C.-C., & RAUDSEPP, M. (2009) Revised values of the bond valence parameters for $^{63}Sb(V)-O$ and $^{121}Sb(III)-O$. *Zeitschrift für Kristallographie* **224**, 423–431.
- POUCHOU, J.L. & PICOIR, F. (1985) 'PAP' $\phi(\rho Z)$ procedure for improved quantitative microanalysis. In *Microbeam analysis* (J.T. Armstrong, ed.). San Francisco Press, San Francisco, California, United States (104–106).
- ROBERTS, A.C., ANSELL, H.G., & DUNN, P.J. (1981) Comancheite, a new mercury oxychloridebromide from Terlingua, Texas. *Canadian Mineralogist* **19**, 393–396.
- ROBERTS, A.C., GRICE, J.D., GAULT, R.A., CRIDDLE, A.J., & ERD, R.C. (1996) Hanawaltite, $Hg^{1+}_6Hg^{2+}[Cl,(OH)]_2O_3$ – A new mineral from the Clear Creek claim, San Benito County, California: Description and crystal structure. *Powder Diffraction* **11**, 45–50.
- ROBERTS, A.C., GROAT, L.A., RAUDSEPP, M., ERCIT, T.S., ERD, R.C., MOFFATT, E.A., & STIRLING, J.A.R. (2001) Clear-creekite, a new polymorph of $Hg^{1+}_3(CO_3)(OH) \cdot 2H_2O$, from the Clear Creek Claim, San Benito County, California. *Canadian Mineralogist* **39**, 779–784.
- ROBERTS, A.C., COOPER, M.A., HAWTHORNE, F.C., CRIDDLE, A.J., STIRLING, J.A.R., & DUNNING, G.E. (2002) Tedhadleyite, $Hg^{2+}Hg^{1+}_{10}O_4I_2(Cl,Br)_2$, a new mineral species from the Clear Creek claim, San Benito County, California. *Canadian Mineralogist* **40**, 909–914.
- ROBERTS, A.C., COOPER, M.A., HAWTHORNE, F.C., GAULT, R.A., GRICE, J.D., & NIKISCHER, A.J. (2003a) Arsmithite, a new Hg^{1+} -Al phosphate-hydroxide from the Funderburk Prospect, Pike County, Arkansas, U.S.A. *Canadian Mineralogist* **41**, 721–725.
- ROBERTS, A.C., COOPER, M.A., HAWTHORNE, F.C., STIRLING, J.A.R., PAAR, W.H., STANLEY, C.J., DUNNING, G.E., & BURNS, P.C. (2003b) Vasilyevite, $(Hg_2)^{2+}_{10}O_6I_3Br_2Cl(CO_3)$, a new mineral species from the Clear Creek

- claim, San Benito County, California. *Canadian Mineralogist* **41**, 1167–1172.
- ROBERTS, A.C., STIRLING, J.A.R., CRIDDLE, A.J., DUNNING, G.E., & SPRATT, J. (2004) Aurivilliusite, $\text{Hg}^{2+}\text{Hg}^{1+}\text{OI}$, a new mineral species from the Clear Creek claim, San Benito County, California, USA. *Mineralogical Magazine* **68**, 241–245.
- ROBERTS, A.C., GAULT, R.A., PAAR, W.H., COOPER, M.A., HAWTHORNE, F.C., BURNS, P.C., CISNEROS, S., & FOORD, E.E. (2005) Terlinguacreekite, $\text{Hg}^{2+}_3\text{O}_2\text{Cl}_2$, a new mineral species from the Perry pit, Mariposa Mine, Terlingua mining district, Brewster County, Texas, U.S.A. *Canadian Mineralogist* **43**, 1055–1060.
- SHELDRIK, G.M. (2008) A short history of *SHELX*. *Acta Crystallographica* **A64**, 112–122.
- STUDEMEISTER, P.A. (1984) Mercury deposits of western California: An overview. *Mineralium Deposita* **19**, 202–207.
- Received December 20, 2018. Revised manuscript accepted March 5, 2019.